IEEE Access
Multidisciplinary | Rapid Review | Open Access Journal

Received November 28, 2019, accepted December 16, 2019, date of publication January 8, 2020, date of current version July 8, 2020.

Digital Object Identifier 10.1109/ACCESS.2020.2964828

Sensorless Loss Model Control of the Six-Phase Induction Motor in All Speed Range by Extended Kalman Filter

ASGHAR TAHERI[1,2], HAI-PENG REN[1], (Member, IEEE), AND MOHAMMAD HOSEIN HOLAKOOIE[2]

[1]School of Electronics and Information Engineering, Xi'an Technological University, Xi'an 710021, China
[2]Electrical Engineering Department, University of Zanjan, Zanjan 4537138791, Iran

Corresponding author: Asghar Taheri (taheri@znu.ac.ir)

This work was supported in part by the Shaanxi Provincial Special Support Program for Science and Technology Innovation Leader, in part by the Shaanxi Industrial Key Project under Grant 2018GY-165, and in part by the Key Laboratory Research Program from Department of Education of Shaanxi Provincial Government under Grant 18JS081.

ABSTRACT This paper proposes a simple extended Kalman filter (EKF) loss model controller (LMC) for efficiency improvement of a six-phase induction machine in all speed ranges. The proposed method is fast and can be operated online. If the machine parameters are changed during the operation, the EKF algorithm is activated to find the parameters to ensure optimal efficiency operation. Not only is the motor speed measurement difficult at low speeds but it is also difficult to calculate the machine efficiency at the same speeds. Thus, the EKF model can estimate speed, load, and motor efficiency at low speed ranges so that optimization can be done in all loads and speed ranges. Unlike the conventional LMC method, the proposed method is independent of parameter variations. Because of the independency of this method against the parameter variations, it works similarly to the search based efficiency control methods. Two DSP boards including estimator and controller are used to achieve high accuracy and speed in estimating and controlling machines. The simulation and experimental results verify the robustness of the sensorless method against parameter variations.

INDEX TERMS EKF, six-phase induction motor, FOC, loss model control.

NOMENCLATURE

$\overrightarrow{\Psi}$	Flux vector
$\overrightarrow{I}$	Current vector
$\overrightarrow{U}$	Voltage vector
T_e, T_l	Electromagnetic and load torque
ω	Electrical rotor speed
s, r	Subscript for stator and rotor quantities
ψ_s, ψ_r	Stator and rotor flux
J	Moment of inertial
R_s, R_r	Stator and rotor resistance
L_s, L_r	Self stator and rotor inductance
T_r	Rotor time constant
T_s	Sample time
M	Magnetizing inductance
P	Number of pole pair
L_{ls}	Stator leakage inductance
X_1, Y_1, U_1	the state vectors of the system
w_1, w_2	the system noises
Q, R, and w_u	Covariance matrices of the system, measurement, and input noise
k_h, ke	Hysteresis and eddy current coefficient

The associate editor coordinating the review of this manuscript and approving it for publication was Chunlong He.

I. INTRODUCTION

Six-phase and five-phase machines are two usual types of multi-phase machines that have several applications [1]–[4]. Increasing machine phases has several advantages, such as higher redundancy and lower torque pulsation. Field-oriented control (FOC) and direct torque control (DTC) techniques are implemented for six-phase and five-phase machines [7]–[11], which speeds up the application of the multiphase machines. These methods cannot achieve good performance in low-speed applications due to the speed measurement difficulty and parameters variation. In low-speed

applications, a suitable method is required to estimate parameters and speed [12]–[14].

The EKF is robust in estimating past, present, and future states of nonlinear systems [25]–[28]. It can be used to estimate various parameters and outputs while there are not any sensors to measure. To estimate the parameters, some of the system outputs are measured by sensors; then, the estimation error is deduced and the Kalman filter coefficients are improved. If the sensors are not accurate enough to measure some parameters, the EKF can be used to improve the accuracy of the measurements [29]–[30]. The Kalman filter and EKF have been used in many research works to estimate motor parameters and outputs of servo systems [31]–[32]. Nowadays, with the increase in processing speed in DSP, the online experiment of EKF has been rendered possible. Induction motors have stochastic properties, so the EKF can easily be used to model it. Also, it can be employed to control machines when they are used at low speeds or the machine parameters are changed. Other estimators are used to estimate the parameters of induction machines [33]–[36].

When a motor operates at a low speed or light load, the system will demonstrate very low efficiency. It is, therefore, essential to use an appropriate method to improve efficiency. The proposed method should be useful at all speed ranges, especially at low-speed ranges. Typically, the efficiency improvement methods of electrical machines are divided into two general categories: loss model control (LMC) [15]–[21] and search control (SC) [22], [23]. Although the SC method is independent of machine parameters, it is time-consuming to implement. Therefore, the SC method cannot be used in highly dynamic applications. In contrast, the LMC technique is relatively fast to implement in a real-time manner; thus, it is suitable for highly dynamic cases, but it depends on machine parameters and offers high computation speed. It is of the practical significance to employ an appropriate method to estimate motor parameters and to improve the LMC method performance. Efficiency improvement of six-phase induction machines has been dealt with in some research papers [23] and [37]. The efficiency improvement method considering highly dynamical applications and all speed ranges of the six-phase induction motors has rarely been reported before to the best knowledge of the authors.

This paper aims to improve the efficiency of a six-phase induction machine (6PIM) in all speed ranges with highly dynamical applications. The EKF is employed to estimate the parameters and states of the motor, which is needed by the LMC to improve the efficiency of the system in the light load conditions. The efficiency improvement method is based on the sensor-less field-oriented control (FOC) framework for 6PIM. The advantage of EKF is not only estimating the speed in the low-speed range with high precision but also estimating the variant parameters, like resistance, to achieve better robustness performance. The innovation of this paper is extending a simple EKF model for 6PIM to achieve high efficiency using the LMC-based FOC of the motor.

In the rest of this paper, a six-phase induction motor modeling and field-oriented control of a 6PIM are first deduced, and EKF modeling of the 6PIM is described in Section II. A suitable loss model control of the 6PIM using the parameters estimated by the EKF is explained in Section III. Finally, extensive simulation results and experiment results are given to validate the correctness of the analysis and the effectiveness of the proposed methods in all speed ranges in Section IV.

II. SIX-PHASE INDUCTION MOTOR MODEL

A. MODELING AND FOC OF MOTOR

The Vector space decomposition (VSD) method is a popular method in the modeling 6PIMs [1]. The technique has been used in several papers as it is simple and suitable for the controller design of 6PIMs. Using this method and applying 6*6 matrices, the six-phase voltage, current, and flux equations are transformed into three subspaces. These subspaces are named $(d-q)$, (z_1-z_2), and (O_1-O_2).

The FOC of the 6PIM is implemented in the $(d-q)$ subspace and the references of the other current subspaces are set to zero. The 6PIM model using the VSD method in that subspace is given below:

$$\overrightarrow{V_s} = R_s\overrightarrow{I_s} + \frac{d\overrightarrow{\Psi_s}}{dt} + j\omega_e\overrightarrow{\Psi_s}, \tag{1}$$

$$0 = R_r\overrightarrow{I_r} + \frac{d\overrightarrow{\Psi_r}}{dt} + j\omega_e'\overrightarrow{\Psi_r}, \omega_e' = \omega_e - \omega_r,$$

$$T_e = 1.5\frac{PM^2}{L_r}i_{ds}i_{qs} = K_{Te}i_{ds}i_{qs}, K_{Te} = 1.5\frac{PM^2}{L_r} \tag{2}$$

According to [32], the dynamic model of the 6PIM in the $(\alpha-\beta)$ subspace can be given as:

$$\begin{cases} X_1^o = A_{c1}(x) + B_{c1}U_1 + w_1, \\ Y_1 = C_{c1}X + w_2 \end{cases} \tag{3}$$

$$X_1 = [I_{s\alpha} \quad I_{s\beta} \quad \Psi_{s\alpha} \quad \Psi_{s\beta}T_l \quad \omega_r R_s], Y_1 = [I_{s\alpha} \quad I_{s\beta}], \quad U_1 = [u_{s\alpha} \quad u_{s\beta}], \tag{4}$$

where X_1, Y_1, and U_1 are the state vector of the system, the measured parameter of the motor, and the input vector in the $(\alpha-\beta)$ subspace, respectively. All noises of the drive system and measurement equipment in that subspace are modeled with w_1 *and* w_2.

$$A_{c1}(x) = \begin{bmatrix} A_{11} & -\omega_r & A_{13} & A_{14}\omega_r & 0 & 0 & 0 \\ \omega_r & A_{22} & A_{23}\omega_r & A_{24} & 0 & 0 & 0 \\ -R_s & 0 & 0 & 0 & 0 & 0 & 0 \\ 0 & -R_s & 0 & 0 & 0 & 0 & 0 \\ -k_T\psi_{sq} & k_T\psi_{sd} & 0 & 0 & 0 & A_{56} & 0 \\ 0 & 0 & 0 & 0 & 0 & 0 & 0 \\ 0 & 0 & 0 & 0 & 0 & 0 & 0 \end{bmatrix} \tag{5}$$

in which

$$A_{11} = A_{22} = -(\frac{R_s}{\sigma L_s} + \frac{R_r}{\sigma L_r}), \quad A_{13} = A_{24} = \frac{R_r}{\sigma L_s M},$$
$$A_{14} = -A_{23} = \frac{\omega_r}{\sigma L_s}, \quad k_T = \frac{3}{2J}, \; A_{56} = \frac{-2}{JP}$$
$$A_{21} = -A_{12} = \omega_r, \quad \sigma = \frac{L_s L_r}{M^2} \tag{6}$$

$$B_{c1} = \begin{bmatrix} \frac{1}{\sigma L_s} & 0 & 1 & 0 & 0 & 0 \\ 0 & \frac{1}{\sigma L_s} & 0 & 0 & 0 & 0 \end{bmatrix}$$
$$C_{c1} = \begin{bmatrix} 1 & 1 & 0 & 0 & 0 & 0 \end{bmatrix} \tag{7}$$

The machine model in the $(z_1 - z_2)$ subspace has only copper loss and it is modeled as follows:

$$\begin{cases} V_{sz1} = R_s I_{sz1} + L_{ls} \frac{d}{dt} I_{sz1} \\ V_{sz2} = R_s I_{sz2} + L_{ls} \frac{d}{dt} I_{sz2} \end{cases} \tag{8}$$

A dynamic model of the 6PIM in the $(z_1 - z_2)$ subspace is

$$\begin{cases} X_2^o = A_{c2}(x) + B_{c2} U_2 + w_1' \\ Y_2 = C_{c2} X + w_2' \end{cases} \tag{9}$$
$$X_2 = [I_{sz1}\, I_{sz2}\, R_s], \; Y_2 = [I_{sz1}\, I_{sz2}]$$
$$U_2 = [u_{sz1}\, u_{sz2}] \tag{10}$$

in which X_2, Y_2, and U_2 denote the state vector of the system, the measured parameter of the motor and the input vector in the $(z_1 - z_2)$ subspace, respectively. All noises of the drive system and measurement equipment in that subspace are modeled with $w_1' and w_2'$.

$$A_{c2} = \begin{bmatrix} -\frac{R_s}{L_s} & 0 & 0 \\ 0 & -\frac{R_s}{L_s} & 0 \\ 0 & 0 & 0 \end{bmatrix}, \quad B_{c2} = \begin{bmatrix} \frac{1}{L_s} & 0 \\ 0 & \frac{1}{L_s} \end{bmatrix},$$
$$C_2 = \begin{bmatrix} 1 & 1 \end{bmatrix}, \tag{11}$$

A discrete model of the motor is needed for the DSP-based digital control of the motor. The discrete model of the 6PIM is deduced by discretizing the state vectors. If the sampling time is T_s, the discrete state vector in the $(\alpha - \beta)$ subspace will be as below

$$\begin{cases} x_1(k) = A_{d1}(x1) x_1(k) + B_{d1}(k) + w_1(k) \\ y_1(k) = C_{d1}(k) + w_2(k) \end{cases} \tag{12}$$

in which $A_{d1}(x1) = A_{c1}(x1)\, T_s + I_{7*7}, B_{d1} = B_{c1} T_s$, $C_{d1} = C_{c1}$

Also, the discrete state vector in the $(z_1 - z_2)$ subspace is:

$$\begin{cases} x_2(k) = A_{d2}(x2) x_2(k) + B_{d2}(k) + w_1'(k) \\ y_2(k) = C_{d2}(k) + w_2'(k) \end{cases} \tag{13}$$

in which $A_{d2}(x2) = A_{c2}(x2)\, T_s + I_{3*3}, B_{d2} = B_{c2} T_s$, $C_{d2} = C_{c2}$

B. EKF MODELING OF 6PIM

When the speed is low, the accuracy of speed sensing and calculation is decreased to a great extent. The EKF is a powerful estimator in this case. The EKF model of the 6PIM is given by recursive equations as below:

$$P(k) = A_{d-d}(\hat{x}(k)) P_h(k) A_{d-d}^T(\hat{x}(k)) + B_{d-d}(u(k)) w_u(k) B_{d-d}^T(u(k)) + Q(k) \tag{14}$$
$$P_h(k+1) = P(k) - P(k) C_d^T(k) (C_d(k) P(k) C_d^T(k) + R)^{-1} C_d(k) P(k) \tag{15}$$
$$\hat{x}_h(k+1) = A_d(\hat{x}) \hat{x}(k) + B_d u^T(k) + P_h(k+1) C_d^T(k) R^{-1} (Y_y' - C_d(k) \hat{x}(k)) \tag{16}$$

in which

$$A_{d-d}(\hat{x}(k)) = \frac{\partial A_d(\hat{x}(k))}{\partial \hat{x}(k)}, \quad B_{d-d}(u(k)) = \frac{\partial B_d(u(k))}{\partial u(k)}$$

where three covariance matrixes (Q, R, and w_u) are used to model the system, measurement, and input noise of the system. These equations are run recursively to decrease the estimation error.

III. LOSS MODELING OF MACHINE

Electrical and mechanical losses are two parts of a drive system. The motor loss decreases the system efficiency and causes the motor temperature to increase. The loss in the machine not only increases the power consumption of the machine but also reduces the operating life of the motor. Electrical motors are designed to have maximum efficiency near the nominal conditions. If a motor load or speed is less than the nominal ones, the motor loss increases. An appropriate method can increase machine efficiency in light load conditions. Previous papers have generally focused on increasing efficiency only under light load conditions, and low speed and light load condition has not been addressed. To this end, a suitable model is used to model the motor losses according to [14].

The total loss of a 6PIM, including stator and rotor copper losses, rotary power loss, and core loss, can be calculated as below [37]:

$$P_{loss} = \frac{1}{2} \left[R_s \left(i_{ds}^2 + i_{qs}^2 \right) + R_r (\frac{L_m}{L_r} i_{qs})^2 \right] + P_{core} + k_m \omega_r^2 \tag{17}$$
$$P_{core} = k_h w_e M^2 I_{sd}^2 + k_e w_e^2 M^2 I_{sd}^2 = p_{c1} + p_{c2} I_{sd}^2 + p_{c3} I_{sd}^{-2}$$
$$p_{c_1} = (k_h + 2 k_e \omega_{rm}) \frac{T_e}{k_{Te}'} M^2, \quad k_{Te}' = k_{Te} T_r$$
$$p_{c_2} = (k_h + k_e \omega_{rm}) M^2 \omega_{rm}$$
$$p_{c_3} = \frac{k_e T_e^2}{k_{Te}'} \tag{18}$$

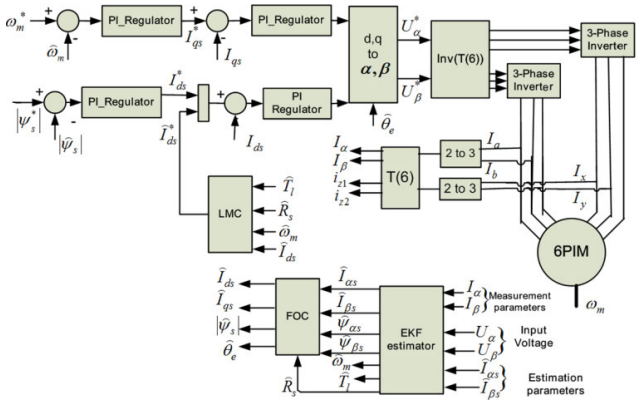

FIGURE 1. The diagram of the EKF based on efficiency improvement in a FOC six-phase induction motor.

From (2), (17), and (18), the total loss is calculated as:

$$P_{loss} = (Ai_{ds}^2 + B\frac{1}{i_{ds}^2} + C) \tag{19}$$

where:

$$A = p_{c_2} + 0.5R_s,$$
$$B = (K_e + \frac{1}{2K'_{Te}} + R_r\frac{L_m^2}{L_r^2K'_{Te}})\frac{T_e^2}{K'_{Te}},$$
$$C = p_{c_3} + k_m\omega_{rm}^2 + \frac{1}{2}\left(R_s\,|i_{sz}|^2 + R_r\,|i_{rz}|^2\right)$$

If the temperature of the machine is increased during the working process, the stator and rotor resistance will be changed. Thus, the loss model control of the machine has many errors. According to Figure 1, the loss model of the machine is calculated from the parameter estimation of the EKF estimator.

$$\hat{P}_{loss} = (\hat{A}i_{ds}^2 + \hat{B}\frac{1}{i_{ds}^2} + \hat{C}) \tag{20}$$

in which $\hat{A}, \hat{B}, \hat{C}, \hat{R}_s, \hat{R}_r, \hat{\omega}_r^2$ represent the estimated parameters of the EKF estimator and are defined as below:

$$\hat{A} = \hat{p}_{c2} + 0.5\hat{R}_s, \quad \hat{p}_{c2} = \left(k_h + k_e\hat{\omega}_{rm}\right)M^2\hat{\omega}_{rm}$$
$$\hat{B} = \left(K_e + \frac{1}{\hat{K}'_{Te}} + \hat{R}_r\frac{L_m^2}{L_r^2\hat{K}'_{Te}}\right)\frac{\hat{T}_e^2}{\hat{K}'_{Te}}$$
$$\hat{C} = \frac{k_e\hat{T}_e^2}{\hat{K}'_{Te}} + k_m\hat{\omega}_{rm}^2 + \frac{1}{2}(\hat{R}_s\,|i_{sz}|^2 + \hat{R}_r\,|i_{sz}|^2)$$

The estimated power differential efficiency optimization of the machine is as below:

$$\frac{\partial P_{loss}}{\partial i_{ds}} = 0 \Rightarrow \hat{I}_{ds}^* = \sqrt[4]{\frac{\hat{B}}{\hat{A}}} \tag{21}$$

which can be used in Figure 1 to achieve efficiency improvement.

IV. SIMULATION AND EXPERIMENTAL RESULTS

In this section, the EKF modeling of a 6PIM at low and high-speed is first shown in Figure 2. In these simulations, the motor speed reference is 1 rad/sec at low speed and 90 rad/sec at high-speed. The EKF algorithm is active and estimates all states. According to this Figure, the load is varied at 1.25 sec to 2 N.m at t = 1.25 sec and then to 1.25 N.m at t = 2.5 sec. Also, the stator resistance is changed from 15 Ω to 25 Ω at t = 3 sec, but the EKF algorithm can estimate these variations.

The simulation is run with and without the LMC algorithm and the results are shown in Figures 3 and 4, respectively. In these figures, the EKF modeling of a 6PIM is active in high-speed and the motor speed reference is 130 rad/sec and load torque is varied. According to results, the load is varied at t = 1.25 sec to 3 N.m and then to 1.25 N.m at t = 3 sec. In figure 3, the LMC algorithm is inactivated and efficiency is low at all load torques. In figure 4, the proposed optimization algorithm is activated after 0.3 sec; thus by changing the load of the 6PIM, the motor currents are varied to the optimal value. Efficiency, input power, motor currents, motor speed, and load torque in the proposed loss model control method are shown in Figure 4(a)–(f). The comparison of Figures 3(a) and 4(a) shows the advantage of the proposed method to improve the efficiency of the 6PIM. According to Figures 3(a) and 4(a), after running the optimization algorithm, the motor efficiency is changed from 13% to 38%. Also, the proposed method increases the motor efficiency from 63% to 64.5% and from 43% to 58% when the load torque is 3 N.m and 1.25 N.m, respectively.

In Figure 5, the LMC is added to the EKF model of the 6PIM at low speed and the efficiency is improved. This Figure illustrates the performance of the proposed algorithm at low speed and load variations. The proposed algorithm is run at 1 second. After running the optimized algorithm, the stator current in the d-axis is changed to the optimal value. while the optimization algorithm is off, the load torque is changed to 0.5 N.m at 2.5 econd. The optimization algorithm is run again at t = 3.5 second while the optimization algorithm is off from t = 5 sec to t = 6 sec, the load torque is changed at 5 sec.

The optimization algorithm is run again at t = 6 second and efficiency is optimized as depicted in Figure 5(a). Also, this figure shows the efficiency improvement, input power, current in the $(\alpha - \beta)$ subspace, rotor flux, load torque, and motor speed in the LMC of the FOC of the 6PIM. The experimental results of the proposed method at a high-speed are displayed in Figure 6. The motor speed is 100 rad/sec and the motor load is 0.5N.m which is changed to 1.5 N.m at t = 1.7 sec. The proposed efficiency improvement algorithm is run at t = 0.8sec and is active until t = 1.7sec. Then, the efficiency improvement is deactivated and run at t = 2.3sec again.

Also, the stator resistance is varied from 15 Ω to 18 Ω at t = 2.7sec. According to the results, the proposed algorithm is active after stator resistance variation and optimal

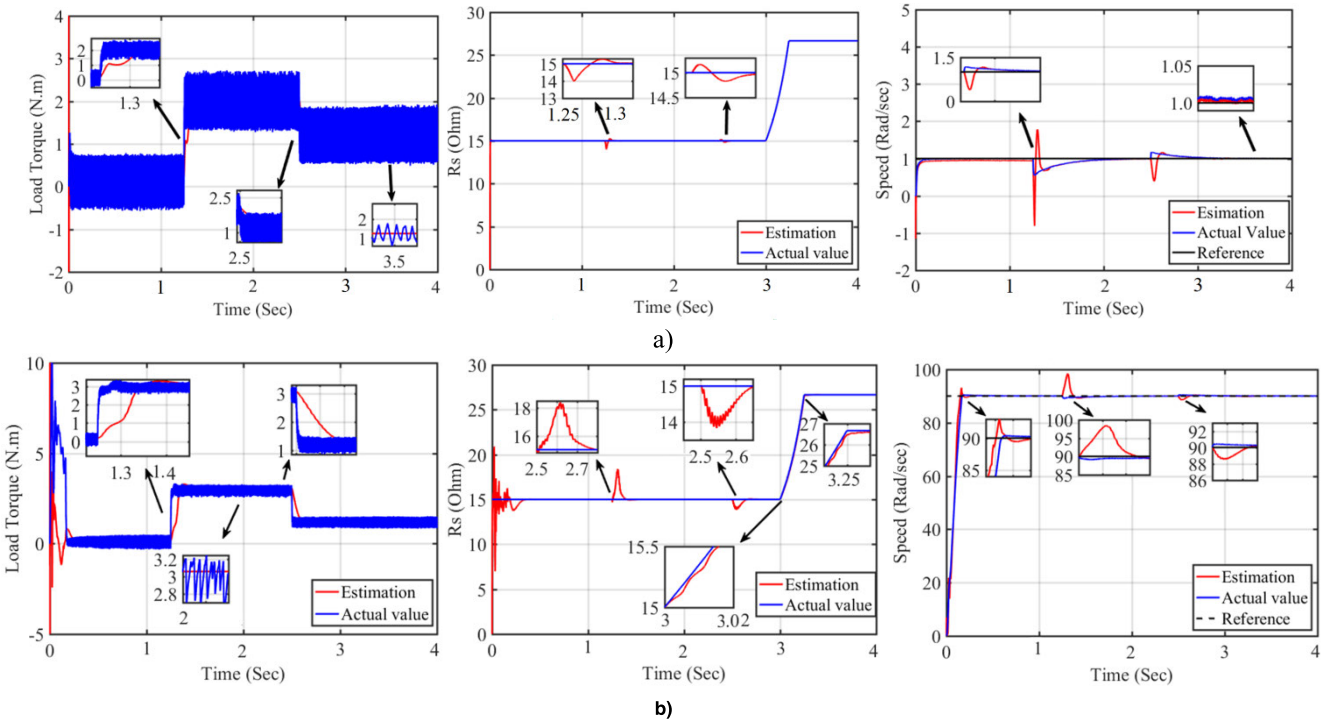

FIGURE 2. The EKF modeling of a six-phase induction motor at a) low-speed, b) high-speed.

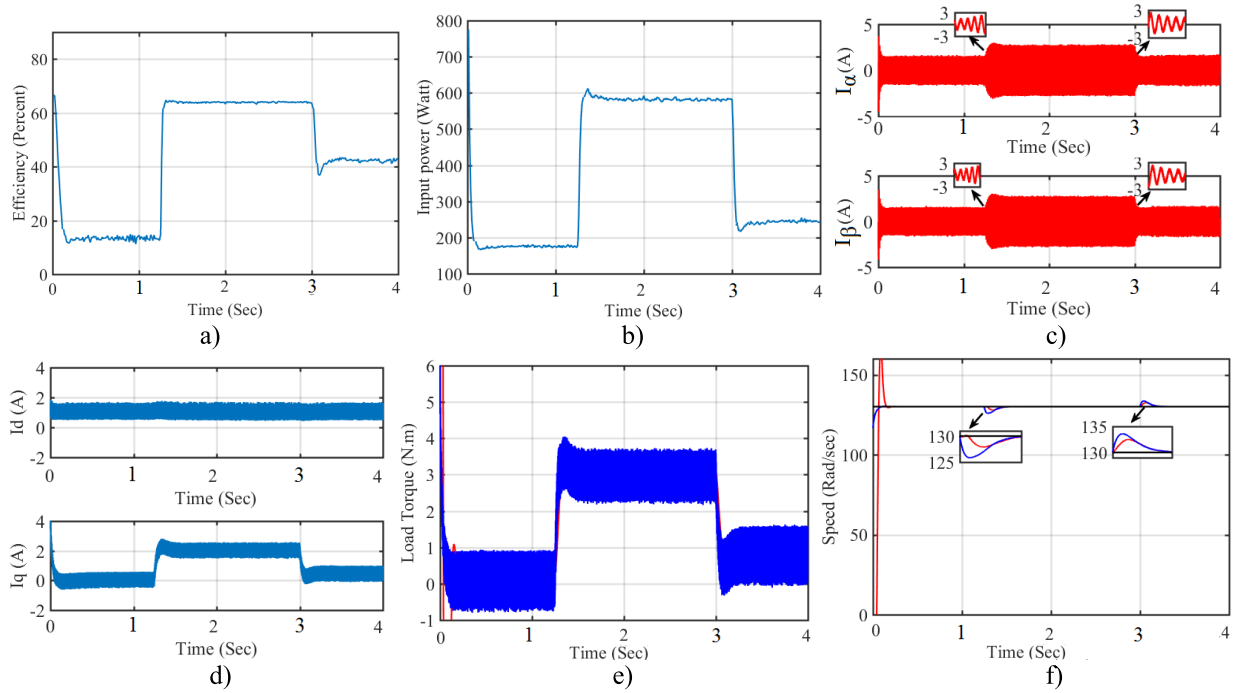

FIGURE 3. The simulation results in high-speed conditions without the loss improvement algorithm, a) efficiency, b) input power, c) current in the ($\alpha - \beta$) subspace, d) d-axis and q-axis current, e) load torque, and f) speed.

efficiency is obtained. Also, the experimental results at low-speed are shown in Figure 7. The motor speed is 1.8 rad/sec and the motor load is varied at t = 2.4 sec. The proposed efficiency improvement algorithm is run at t = 0.8sec and is active until the load change. Then, the efficiency improvement is deactivated and run at t = 3.4 sec again.

Besides, the stator resistance is varied from 15Ω to 18Ω at t = 3.9 sec. According to the results, the proposed algorithm

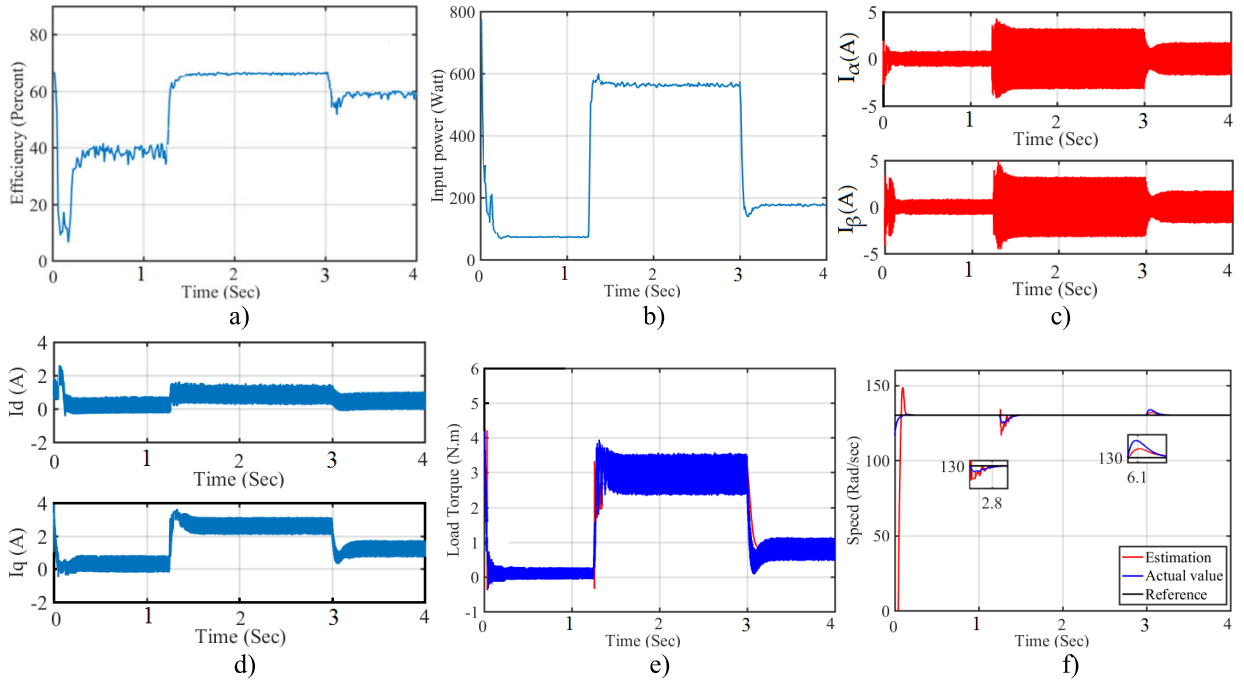

FIGURE 4. The simulation results in high speed conditions without the loss improvement algorithm, a) efficiency, b) input power, c) current in the ($\alpha - \beta$) subspace, d) d-axis and q-axis current, e) load torque, and f) speed.

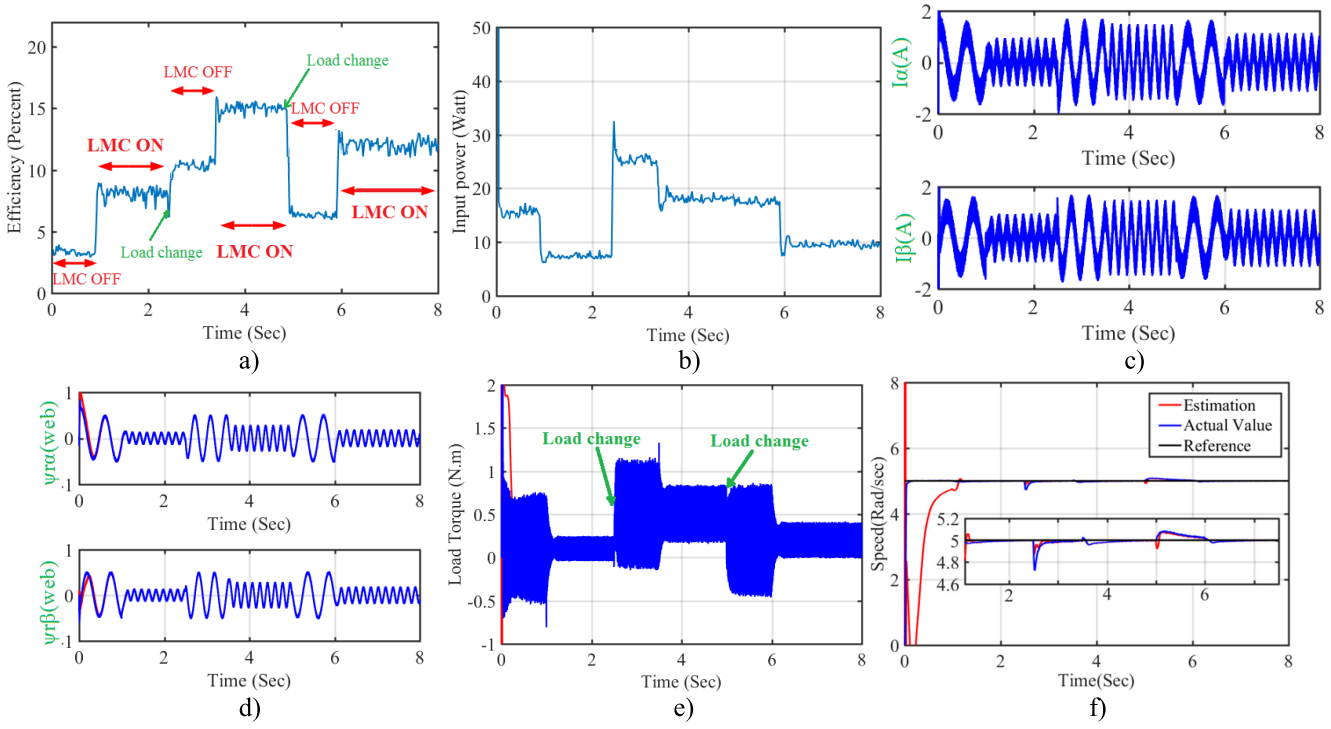

FIGURE 5. The simulation results in low-speed conditions with the loss improvement algorithm, a) efficiency, b) input power, c) current in the ($\alpha - \beta$) subspace, d) rotor flux e) load torque, and f) motor speed.

is active at all speed ranges and can minimize the power loss very fast. In addition, the proposed method is independent of parameter variations and optimal efficiency is obtained with parameter variations.

The proposed technique to improve efficiency has been developed and tested in an experimental set-up. The structure of the implemented hardware is illustrated in Figure 8. The test-bench is composed of a 6PIM and load. This machine

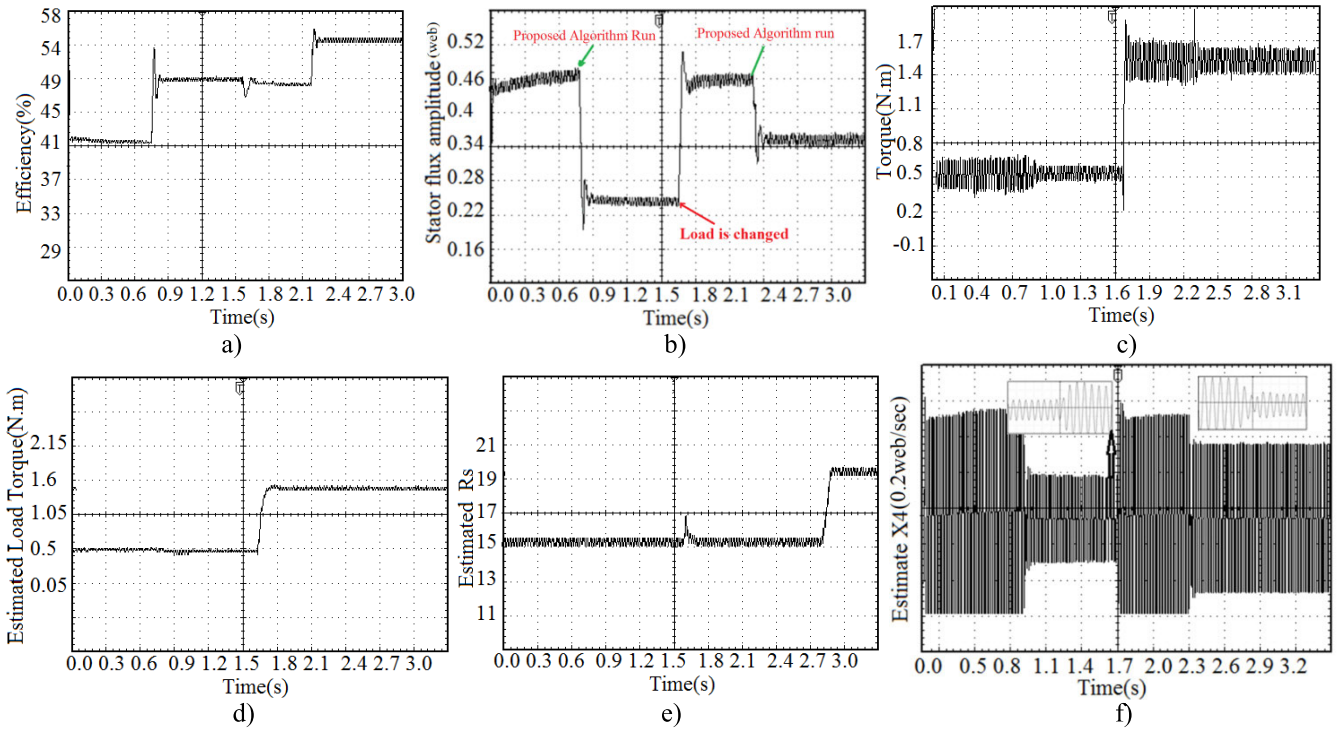

FIGURE 6. The experimental results of LMC of a six-phase induction motor by EKF at a high-speed and when Rs is changed, a) efficiency, b) stator flux, c) torque, d) estimated load torque, e) estimated Rs, and f) estimated $\psi_{s\beta}$.

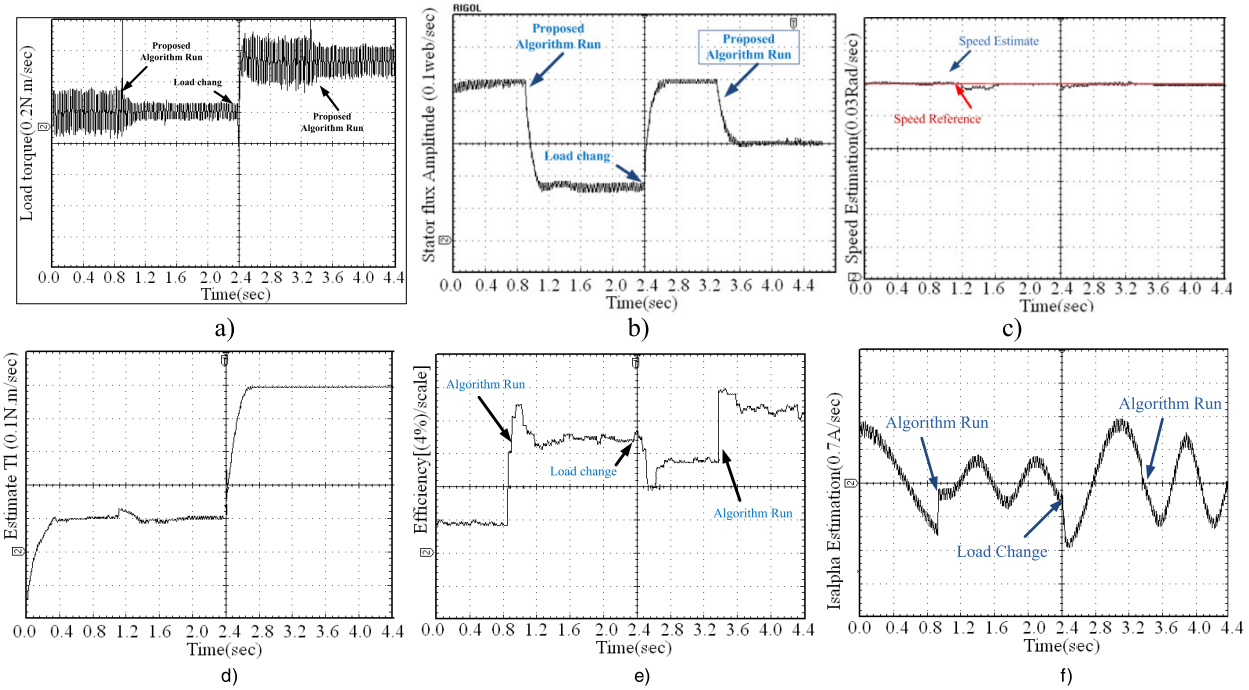

FIGURE 7. Results of LMC of a six-phase induction motor by EKF at a low-speed, a) load torque, b) estimated stator flux amplitude, c) estimated speed, d) estimated load torque, e) estimated efficiency, and f) estimated $\psi_{s\beta}$.

is fed by a six-phase DC-AC VSI. The 6PIM is made of a three-phase induction motor by rewinding the stator as an asymmetrical structure. The motor specification parameters are shown in Table 1.

To perform the 6PIM closed-loop vector control, the six stator phase currents are sensed using LEM current sensors. Four current sensors are used to measure the phase currents of VSI. The outputs of sensors

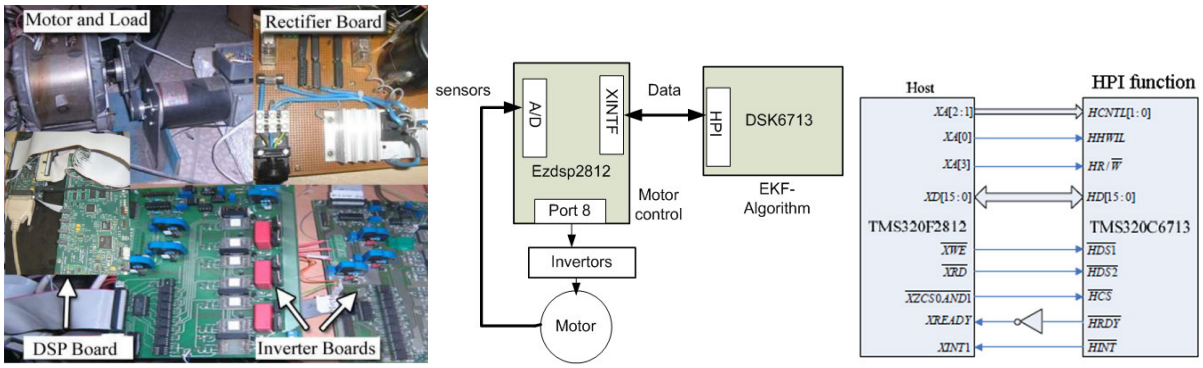

FIGURE 8. The experimental setup.

TABLE 1. Motor specifications.

L_m	589.1mH	R_s	15.0 Ω
L_s	603.3mH	R_r	7.91 Ω
L_r	604.3mH	$J_{Motor\&Load}$	5.2*10-3 kgm2
Rated speed	150 rad/sec	Motor power	750w

TABLE 2. Compare of efficiency improvement of various methods without parameter changes.

Load Torque (N.m)	Efficiency before LMC(%)	Efficiency of Proposed method (%)	Efficiency with [38] (%)	Efficiency with [39] (%)
0.3	13	38	36.3	34
3	63	66.5	65.9	65.1
1.25	43	59	57.8	56.6

TABLE 3. Compare of efficiency improvement of various methods with 30% stator resistance variations.

Load Torque (N.m)	Efficiency before LMC (%)	Efficiency of proposed method (%)	Efficiency with [38] (%)	Efficiency with [39] (%)
0.3	13	37.1	28.3	26.2
3	63	65.9	57.3	56.1
1.25	43	58.2	48.2	49.6

are digitized using six 12-bit A/Ds in the TMS board.

TMS3206713 is a floating point processor with 225 MHZ clock time that can execute real-time algorithms. Tms320F2812, which is a fixed point microcontroller, has favorable performance in motor control by useful peripherals. If the control and estimation algorithms are implemented in one DSP board, the execution time and sampling time will be large. To reduce sampling time, the control algorithm is implemented in EZDSP2812 board and the EKF algorithm is implemented in the DSK6713 board.

For the high-speed interface of two DSP boards, a parallel interface is used. To this end, an HPI port in DSK6713 is connected to P2 (XINTF) in EZDSP2812. The host port interface (HPI) is a parallel port in DSK6713 for rapidly sending and receiving data. The host processor can directly access the CPU memory space by the HPI port.

The proposed loss model control method has been compared with other power loss minimization strategies. Table 2 summarizes the improvements caused by some of the methods available in the literature. In this table, the announced results are the average values for load torque, efficiency before loss minimization, and efficiency after loss minimization methods with different load torques.

According to table 2, the proposed loss minimization method has a good response in low load conditions than other methods. Also, if the stator resistance is varied the proposed method can estimate the optimal current very well. Compare of efficiency improvement of various methods with 30% stator resistance variations are shown in Table 3. According to the results, the proposed method has the best response in various loads. If motor parameters are changed without parameter estimation, the motor efficiency is decreased.

V. CONCLUSION

The EKF loss model control of a 6PIM presented in this paper gives optimal efficiency at all speed ranges. According to the results, the proposed method is active under load variations and the variations of parameters. If the motor speed is low, the proposed method estimates the speed and optimal flux to reduce the loss and improve efficiency. Also, the proposed method is fast and can estimate machine parameters and motor loss online. The proposed method is independent of parameter variations and optimal efficiency is obtained with parameter variations. This technique has some the advantage against the usual efficiency improvement methods. This method is as fast as the LMC method and the proposed method is independent of motor parameters like the SC techniques. The performance of the proposed method is proven with simulations and experimental results perfectly.

ABBREVIATIONS

EKF	Extended Kalman filter
LMC	Loss model controller
FOC	Field-oriented control
DTC	Direct torque control
SC	Search control
6PIM	Six-phase induction machine
VSD	Vector space decomposition
VSI	Voltage source inverter
HPI	Host port interface

REFERENCES

[1] W. N. W. A. Munim, M. J. Duran, H. S. Che, M. Bermudez, I. Gonzalez-Prieto, and N. A. Rahim, "A unified analysis of the fault tolerance capability in six-phase induction motor drives," *IEEE Trans. Power Electron.*, vol. 32, no. 10, pp. 7824–7836, Oct. 2017.

[2] A. S. Abdel-Khalik, M. S. Hamad, A. M. Massoud, and S. Ahmed, "Post-fault operation of a nine-phase six-terminal induction machine under single open-line fault," *IEEE Trans. Ind. Electron.*, vol. 65, no. 2, pp. 1084–1096, Feb. 2018.

[3] M. Qiao, C. Jiang, Y. Zhu, and G. Li, "Research on design method and electromagnetic vibration of six-phase fractional-slot concentrated-winding PM motor suitable for ship propulsion," *IEEE Access*, vol. 4, pp. 8535–8543, 2016.

[4] S. M. Suhel and R. Maurya, "Realization of 24-sector SVPWM with new switching pattern for six-phase induction motor drive," *IEEE Trans. Power Electron.*, vol. 34, no. 6, pp. 5079–5092, Jun. 2019.

[5] A. S. Abdel-Khalik, R. A. Hamdy, A. M. Massoud, and S. Ahmed, "Post-fault control of scalar (V/f) controlled asymmetrical six-phase induction machines," *IEEE Access*, vol. 6, pp. 59211–59220, 2018.

[6] T. S. De Souza, R. R. Bastos, and B. J. C. Filho, "Modeling and control of a nine-phase induction machine with open phases," *IEEE Trans. Ind. Appl.*, vol. 54, no. 6, pp. 6576–6585, Nov. 2018.

[7] R. Bojoi, M. Lazzari, F. Profumo, and A. Tenconi, "Digital field-oriented control for dual three-phase induction motor drives," *IEEE Trans. Ind. Appl.*, vol. 39, no. 3, pp. 752–760, May 2003.

[8] R. Bojoi, F. Farina, A. Tenconi, F. Profumo, and E. M. Levi, "Dual three-phase induction motor drive with digital current control in the stationary reference frame," *IEE Proc.-Electr. Power Appl.*, vol. 20, no. 3, pp. 40–43, June/Jul. 2006.

[9] K. Mohapatra, R. Kanchan, M. Baiju, P. Tekwani, and K. Gopakumar, "Independent field-oriented control of two split-phase induction motors from a single six-phase inverter," *IEEE Trans. Ind. Electron.*, vol. 52, no. 5, pp. 1372–1382, Oct. 2005.

[10] A. S. Abdel-Khalik, R. A. Hamdy, A. M. Massoud, and S. Ahmed, "Low-order space harmonic modeling of asymmetrical six-phase induction machines," *IEEE Access*, vol. 7, pp. 6866–6876, 2019.

[11] H. Masoumkhani and A. Taheri, "PI regulator-based duty cycle control to reduce torque and flux ripples in DTC of six-phase induction motor," *IEEE J. Emerg. Sel. Topics Power Electron.*, early access, doi:10.1109/jestpe.2018.2889240 .

[12] M. H. Holakooie, M. Ojaghi, and A. Taheri, "Direct torque control of six-phase induction motor with a novel MRAS-based stator resistance estimator," *IEEE Trans. Ind. Electron.*, vol. 65, no. 10, pp. 7685–7696, Oct. 2018.

[13] A. Pantea, A. Yazidi, F. Betin, S. Carriere, A. Sivert, B. Vacossin, H. Henao, and G.-A. Capolino, "Fault-tolerant control of a low-speed six-phase induction generator for wind turbines," *IEEE Trans. Ind. Appl.*, vol. 55, no. 1, pp. 426–436, Jan. 2019.

[14] J. Lavenius and L. Vanfretti, "PMU-based estimation of synchronous machines' unknown inputs using a nonlinear extended recursive three-step smoother," *IEEE Access*, vol. 6, pp. 57123–57136, 2018.

[15] M. Uddin and S. W. Nam, "New online loss-minimization-based control of an induction motor drive," *IEEE Trans. Power Electron.*, vol. 23, no. 2, pp. 926–933, Mar. 2008.

[16] S. Yamamoto, H. Hirahara, J. B. Adawey, T. Ara, and K. Matsuse, "Maximum efficiency drives of synchronous reluctance motors by a novel loss minimization controller with inductance Estimator," *IEEE Trans. Ind. Appl.*, vol. 49, no. 6, pp. 2543–2551, Nov. 2013.

[17] D. Zhi, L. Xu, and B. Williams, "Model-based predictive direct power control of doubly fed induction generators," *IEEE Trans. Power Electron.*, vol. 25, no. 2, pp. 341–351, Feb. 2010.

[18] S. Di Gennaro, J. R. Dominguez, and M. A. Meza, "Sensorless high order sliding mode control of induction motors with core loss," *IEEE Trans. Ind. Electron.*, vol. 61, no. 6, pp. 2678–2689, Jun. 2014.

[19] J.-F. Stumper, A. Dotlinger, and R. Kennel, "Loss minimization of induction machines in dynamic operation," *IEEE Trans. Energy Convers.*, vol. 28, no. 3, pp. 726–735, Sep. 2013.

[20] M. G. Bijan and P. Pillay, "Efficiency estimation of the induction machine by particle swarm optimization using rapid test data with range constraints," *IEEE Trans. Ind. Electron.*, vol. 66, no. 8, pp. 5883–5894, Aug. 2019.

[21] E. B. Agamloh, A. Cavagnino, and S. Vaschetto, "Standard efficiency determination of induction motors with a PWM inverter source," *IEEE Trans. Ind. Appl.*, vol. 55, no. 1, pp. 398–406, Jan. 2019.

[22] G. Hong, T. Wei, and X. Ding, "Multi-objective optimal design of permanent magnet synchronous motor for high efficiency and high dynamic performance," *IEEE Access*, vol. 6, pp. 23568–23581, 2018.

[23] A. Taheri, A. Rahmati, and S. Kaboli, "Efficiency improvement in DTC of six-phase induction machine by adaptive gradient descent of flux," *IEEE Trans. Power Electron.*, vol. 27, no. 3, pp. 1552–1562, Mar. 2012.

[24] A. Mohammadpour and L. Parsa, "A unified fault-tolerant current control approach for five-phase PM motors with trapezoidal back EMF under different stator winding connections," *IEEE Trans. Power Electron.*, vol. 28, no. 7, pp. 3517–3527, Jul. 2013.

[25] C. M. Verrelli, A. Savoia, M. Mengoni, R. Marino, P. Tomei, and L. Zarri, "On-line identification of winding resistances and load torque in induction machines," *IEEE Trans. Control Syst. Technol.*, vol. 22, no. 4, pp. 1629–1637, Jul. 2014.

[26] F. Alonge, T. Cangemi, F. D'Ippolito, A. Fagiolini, and A. Sferlazza, "Convergence analysis of extended Kalman filter for sensorless control of induction motor," *IEEE Trans. Ind. Electron.*, vol. 62, no. 4, pp. 2341–2352, Apr. 2015.

[27] M. Barut, R. Demir, E. Zerdali, and R. Inan, "Real-time implementation of bi input-extended Kalman filter-based estimator for speed-sensorless control of induction motors," *IEEE Trans. Ind. Electron.*, vol. 59, no. 11, pp. 4197–4206, Nov. 2012.

[28] G. Edelbaher, K. Jezernik, and E. Urlep, "Low-speed sensorless control of induction machine," *IEEE Trans. Ind. Electron.*, vol. 53, no. 1, pp. 120–129, Feb. 2006.

[29] Y. Li, J. Li, J. Qi, and L. Chen, "Robust cubature Kalman filter for dynamic state estimation of synchronous machines under unknown measurement noise statistics," *IEEE Access*, vol. 7, pp. 29139–29148, 2019.

[30] X.-L. Yang, G.-R. Liu, N.-H. Chen, and T.-S. Lou, "Desensitized ensemble Kalman filtering for induction motor estimation," *IEEE Access*, vol. 7, pp. 78029–78036, 2019.

[31] D. E. G. Erazo, O. Wallscheid, and J. Bocker, "Improved fusion of permanent magnet temperature estimation techniques for synchronous motors using a Kalman filter," *IEEE Trans. Ind. Electron.*, vol. 67, no. 3, pp. 1708–1717, Mar. 2020.

[32] H. Al-Ghossini, F. Locment, M. Sechilariu, L. Gagneur, and C. Forgez, "Adaptive-tuning of extended Kalman filter used for small scale wind generator control," *Renew. Energy*, vol. 85, pp. 1237–1245, Jan. 2016.

[33] A. Taheri, "EKF modeling of field oriented control of six-phase induction motor," *IEICE Electron. Express* vol. 9, no. 7, pp. 642–647, 2012.

[34] G. Feng, C. Lai, J. Tjong, and N. C. Kar, "Noninvasive Kalman filter based permanent magnet temperature estimation for permanent magnet synchronous machines," *IEEE Trans. Power Electron.*, vol. 33, no. 12, pp. 10673–10682, Dec. 2018.

[35] J. K. Pandit, M. V. Aware, R. V. Nemade, and E. Levi, "Direct torque control scheme for a six-phase induction motor with reduced torque ripple," *IEEE Trans. Power Electron.*, vol. 32, no. 9, pp. 7118–7129, Sep. 2017.

[36] A. Taheri, A. Rahmati, and S. Kaboli, "Energy optimization of field oriented six-phase induction motor drive," *Adv. Elect. Comput. Eng.*, vol. 11, no. 2, pp. 107–112, 2011.

[37] M. H. Holakooie, M. Ojaghi, and A. Taheri, "Modified DTC of a six-phase induction motor with a second-order sliding-mode MRAS-based speed Estimator," *IEEE Trans. Power Electron.*, vol. 34, no. 1, pp. 600–611, Jan. 2019.

[38] H. A. Zarchi, H. M. Hesar, and M. A. Khoshhava, "Online maximum torque per power losses strategy for indirect rotor flux-oriented control-based induction motor drives," *IET Electr. Power Appl.*, vol. 13, no. 2, pp. 259–265, Feb. 2019.
[39] M. Farasat, A. M. Trzynadlowski, and M. S. Fadali, "Efficiency improved sensorless control scheme for electric vehicle induction motors," *IET Electr. Syst. Transp.*, vol. 4, no. 4, pp. 122–131, Dec. 2014.

ASGHAR TAHERI was born in Zanjan, Iran, in 1977. He received the B.S., M.S., and Ph.D. degrees in electronics engineering from the Amirkabir University of Technology and the Iran University of Science and Technology, Tehran, Iran, in 1999, 2002, and 2011, respectively. He has been a member of the Faculty at the University of Zanjan, Iran, since 2010, where he was an Assistant Professor, from 2011 to 2016, and has been an Associate Professor, since 2016. He was a Visiting Professor with the University of Alberta, Canada, from January 2019 to April 2019, and then, he joined to Xi'an Technological University. His current research interests include modeling, analysis, and control of power converters, motor drives and control, and multiphase machine drives, multilevel inverter, power electronic systems for renewable energy sources, process control, DSP and FPGA-based system designs, hardware in the loop, and computer-aided control.

HAI-PENG REN (Member, IEEE) was born in Heilongjiang, China, in 1975. He received the Ph.D. degree in power electronics and power drives from the Xi'an University of Technology, in 2003. He was a Visiting Researcher in the field of nonlinear phenomenon of power converters with Kyushu University, Japan, from April 2004 to October 2004. He was a Post Ph.D. Research Fellow in the field of time-delay system with Xi'an Jiaotong University, from 2005 to 2008. He was a Honorary Visiting Professor in the field of communication with chaos and complex networks with the University of Aberdeen, Scotland, from July 2010 to July 2011. Since 2018, he has been a Professor with the Department of Information and Control Engineering, Xi'an University of Technology, Xi'an, China. In June 2018, he moved to Xi'an Technological University. His research fields include nonlinear system control, complex networks, and communication with nonlinear dynamics.

MOHAMMAD HOSEIN HOLAKOOIE was born in Tehran, Iran, in 1989. He received the B.Sc. degree in electrical engineering from Guilan University, Rasht, Iran, in 2011, and the M.Sc. degree in electrical engineering from Tabriz University, Tabriz, Iran, in 2013. He is currently pursuing the Ph.D. degree in electrical engineering with Zanjan University, Zanjan, Iran. His current research interest includes analysis and control of rotary and linear electric machines.